ENERGY PRINCIPLE WITH GLOBAL INVARIANTS: APPLICATIONS

by

A. Bhattacharjee,
R.L. Dewar[a], A.H. Glasser[b], M.S. Chance[a], and J.C. Wiley[c]

Institute for Fusion Studies
University of Texas at Austin, Austin, Texas 78712

ABSTRACT

Minimum-energy equilibrium states of a pressureless cylindrical plasma are constructed subject to a recently proposed set of constraints appropriate to turbulent relaxation dominated by a tearing mode of single helicity. Stability to ideal and resistive modes is examined. It is found that the relaxed states of minimum energy are always stable to the dominant mode, as well as a class of other low m and n modes, but that there are typically high n residual instabilities in the case of the pinch branch, and a residual m=3, n=2 resistive instability is found for an otherwise stable narrow window in the tokamak branch. It is argued that the residual instabilities may be compatible with experimental observations.

---

[a]Plasma Physics Laboratory, Princeton University, Princeton, New Jersey, 08544

[b]Auburn University, Auburn, Alabama 36849

[c]Fusion Research Center, University of Texas at Austin, Austin, Texas 78712

I. Introduction

In two recent papers[1],[2] (hereafter referred to as Papers I and II), we have proposed a variational principle for constructing equilibria with minimum energy in slightly nonideal plasmas. In this principle, the total energy of a plasma is minimized subject to global invariants which are preserved exactly by all ideal motions and approximately, by a certain class of nonideal motions. The precise extent of the class of nonideal motions is designated by a model of magnetic reconnection due to Kadomtsev[3] and Monticello, which describes the nonlinear evolution of a tearing mode of single helicity. The motivation for constructing equilibria in such a fashion is that it should lead to equlibria which are at once ideally and resistively stable, provided, of course, it is possible to determine an optimum set of global invariants.

In the classic variational principle of Kruskal and Kulsrud[4], each member of a complete class of static equilibria is characterized by a nondenumerable set of topological invariants. Taylor[5] has conjectured that for a toroidal plasma of volume V_0 confined by a magnetic field $\vec{B}$($\vec{B} = \vec{\nabla} \times \vec{A}$, where $\vec{A}$ is the vector potential), the ideal global invariant,

$$K_0 = \int_{V_0} d\tau \, \frac{\vec{A} \cdot \vec{B}}{2} \quad , \tag{1}$$

originally due to Woltjer and Moffatt, is the only invariant that is preserved approximately in the presence of a small amount of resistivity. The Euler-Lagrange equation for extrema of the magnetic energy

$$W = \int_{V_0} d\tau \, \frac{B^2}{2} , \tag{2}$$

subject to the constancy of K_0 is

$$\vec{J} = \lambda_0 \vec{B} , \tag{3}$$

where λ_0 is a Lagrange multiplier.

In Papers I and II, on the basis of the Kadomtsev-Monticello model, we have attempted to provide a mechanism for the invariance of K_0. We have concluded (see, for instance, Sec. V of Paper II) plausibly that if tearing modes of different helicities are strongly coupled to one another, the only surviving invariant is K_0. In the light of this conclusion, it is perhaps not surprising that Taylor's theory has provided a good explanation for self-reversal in a device such as Zeta in which, for slow rise-time of the current, virulent tearing activity often developed into turbulence[6]. Unfortunately, for tokamaks, in which the toroidal field B_z is approximately constant, Eq. (2) requires that the current J_z be flat across the entire section of the plasma, which happens only in the event of a major disruption when a large fraction of the magnetic energy of the plasma is suddenly released and a sharp negative spike is recorded in the loop voltage. In particular, the work of Waddell, Carreras, Hicks and Holmes[7] has demonstrated that a sufficient condition for a major disruption is provided by the strong nonlinear interaction between the m=2, n=1 mode and higher harmonics, particularly odd modes such as the m=3, n=2 mode. Most of the time, such strong interaction is avoided in a typical tokamak discharge. We are therefore led to the conclusion that during a reasonably well-confined tokamak discharge, K_0 is not the only surviving invariant.

In Paper II, we have conjectured that in a slightly nonideal tokamak plasma, where modes often coexist without strong coupling to one another, the best preserved invariants are K_0 and

$$K_1 = \int_{V_0} d\tau \, \chi \frac{\vec{A}\cdot\vec{B}}{2} , \tag{4}$$

where χ is the helical flux function corresponding to the dominant mode of pitch q_s. Imposing additional constraints on the system has the obvious effect of increasing its potential energy. Knowing that Taylor's theory leads to equilibria which are too low in energy to be of interest for tokamaks, we have attempted to construct equilibria with a minimum number of additional constraints; enough, however, to reproduce essential features of a well-confined tokamak discharge.

We represent the magnetic field $\vec{B}$ by

$$\vec{B} = \vec{\nabla}\zeta \times \vec{\nabla}\Psi + \vec{\nabla}\Phi \times \vec{\nabla}\theta , \tag{5}$$

where the poloidal flux function Ψ labels flux surfaces radially, θ and ζ are, respectively, the poloidal and toroidal angles parametrizing a flux surface and Φ is the toroidal flux function. Then, the helical flux function χ is given by

$$\chi = q_s\Psi - \Phi . \tag{6}$$

We adopt the boundary conditions

$$\Psi = 0 , \tag{7}$$

on the conducting wall bounding the plasma and

$$\Phi = 0, \tag{8}$$

on the magnetic axis. The boundary condition (8) makes $2\pi\Phi_p$ the total toroidal flux, which is a globally conserved quantity in this theory. It is convenient to choose a gauge such that

$$\vec{A} = \Phi\vec{\nabla}\theta - \Psi\vec{\nabla}\zeta \ . \tag{9}$$

Minimizing W subject to the invariants K_0 and K_1, we obtain the Euler-Lagrange equation

$$\vec{J} = \left[\lambda_0 + \frac{3\lambda_1}{2}\chi\right] \vec{B} \ , \tag{10}$$

derived in Paper II. Since we are primarily interested in equilibria which may be sustained on the transport timescale, beyond the timescale of relaxation due to tearing instabilities, we examine those solutions of Eq. (10) for which $\vec{J}$ vanishes on the wall. These equilibria are obtained by requiring that

$$\frac{3\lambda_1}{2} = \frac{\lambda_0}{\Phi_p} \ , \tag{11}$$

where Φ_p is the value of Φ on the wall. Then the equilibrium Eq. (10) reduces to

$$\vec{J} = \lambda_0 \left[1 + \frac{q_s\Psi - \Phi}{\Phi_p}\right] \vec{B} \ . \tag{12}$$

It is to be noted that solutions of Eq. (3) (obtained in Taylor's

theory) have, in general, nonvanishing $\vec{J}$ on the edge of the plasma, in obvious disagreement with experimental observations of the toroidal current which is usally small near the edge.

There is yet another crucial aspect of the equilibria described by Eq. (3) which deserves comment. In cylindrical geometry (r,θ,z), assuming that equilibrium quantities depend only on r, it is well known that the driving term for tearing modes is $d\sigma/dr$, where

$$\sigma \equiv \frac{\vec{J} \cdot \vec{B}}{B^2} \quad . \tag{13}$$

We note that for equilibria given by Eq. (3),

$$\frac{d\sigma}{dr} = 0 \quad , \tag{14}$$

which, for a plasma bounded by a conducting wall, is an overkill for the problem of instability. In fact, it is because equilibria obeying Eq. (14) are unrealistic, that much effort has been expended in constructing stable equilibria for tokamaks[8] as well as reversed-field pinches by optimizing current profiles for which $d\sigma/dr$ is not generally zero. We emphasize that $d\sigma/dr \neq 0$ for the equilibrium Eq. (12) derived from the present theory.

This paper is divided into three main sections. Section II contains detailed solutions in cylindrical geometry of the equilibrium equation derived from the variational principle. We describe the tokamaklike and pinchlike solutions of the equilibrium equation, which we solve in asymptotic limits to explain the numerical solutions. In Sec. III, we compare the predictions of our theory with experimental data on self-reversal in pinches. In Sec. IV, we investigate the ideal and resistive

stability of the equilibria of minimum energy derived from the variational principle.

II. Equilibrium Solutions in Cylindrical Geometry

A toroidal device of large aspect ratio may be simulated by a straight cylinder of radius a and periodicity length $2\pi R$. In cylindrical polar coordinates (r,θ,z), if we assume that equilibrium quantities depend only on r, and define $\underline{\underline{\bar{B}}} = \vec{B}/2\Phi_p$, $\bar{\Psi} = q_s\Psi/2\Phi_p$ and $\bar{\Phi} \equiv \Phi/2\Phi_p$, we may write Eq. (12) and the accompanying boundary conditions as the two-point boundary-value system,

$$\bar{B}_r = 0 \ , \tag{15a}$$

$$\frac{d\bar{B}_z}{dr} = -\lambda_0 \bar{B}_\theta \ \left[1 + 2(\bar{\Psi}-\bar{\Phi})\right] \ , \tag{15b}$$

$$\frac{1}{r}\frac{d}{dr}(r\bar{B}_\theta) = \lambda_0 \bar{B}_z \ \left[1 + 2(\bar{\Psi}-\bar{\Phi})\right], \tag{15c}$$

$$\frac{d\bar{\Psi}}{dr} = q_s R \ \bar{B}_\theta \ , \tag{15d}$$

$$\frac{d\bar{\Phi}}{dr} = r \ \bar{B}_z \ , \tag{15e}$$

$$\bar{B}_\theta(0) = 0,\ \bar{\Psi}(1) = 0,\ \bar{\Phi}(0) = 0,\ \bar{\Phi}(1) = 1/2, \tag{15f}$$

where we have asusmed for convenience that the radius a = 1.

We note that the solutions to the system of Eqs. (15) depend on q_s and R only through the product q_sR. In Paper I, we have argued that the growth and subsequent decay of the fastest growing tearing mode provides the mechanism responsible for the breaking of most but not all of the infinity of ideal constraints. From linear and nonlinear theories of tokamak stability[10], we know that the m=1, n=1 tearing mode grows much faster than the m≥2, n=1 modes. Also, there is experimental evidence on the PLT tokamak that discharges in the so-called "internal sawtooth" regime, in which the plasma dominantly exhibits "soft" m=1, n=1 activity uncoupled to weak higher harmonics, is particularly good for confinement. We shall, therefore, at first discuss the solutions to Eqs. (15) assuming the dominant mode to be m=1, n=1 (q_s=1), given its importance for tokamaks. We shall see later, however, that if we confine ourselves to the small class of modes usually observed by experimentalists, the qualitative features of this theory are not very sensitive to the choice of a particular dominant mode.

The system of Eqs. (15) has been solved numerically by a shooting procedure. For a cylinder of aspect ratio R/a = 5 (q_sR=5), these results (which were published in our earlier paper but are reproduced here for a more detailed discussion) may be best understood by reference to Fig. 1 which shows a plot of $V(\lambda_0) \equiv 2R^{-1}(2\pi\Phi_p)^{-2}W(\lambda_0)$ versus $R^{-1}K_0(\lambda_0)(2\pi\Phi_p)^{-2}$. There are two classes of solutions, which we have broadly classified as "pinchlike" (P) and "tokamaklike" (T). The reason for this nomenclature is that these two classes contain "windows" of minimum energy for which the q-profiles are repectively monotonically decreasing and increasing; however, there are

solutions on both of these branches for which the q-profiles are not monotonic. For a given value of $R^{-1}K_0(\lambda_0)\ (2\pi\Phi_p)^{-2}$, which is proportional to the amount of volt-seconds/toroidal flux in the system, the plasma should prefer the states of lower energy indicated by the solid lines in Fig. 1. The dashed lines indicate equilibria for which W is stationary but not a global minimum. In fact, if experimental conditions should drive the plasma to the states of higher energy indicated by the dashed lines, instabilities would presumably develop and force the plasma to states of lower energy. We compare the energy of the equilibria permitted by Eqs. (15) to the energy of the axisymmetric equilibria in Taylor's theory. As expected, the imposition of the additional invariant K_1 over and above those imposed by Taylor raises the energy of the system for the same value of the constraint.

The arrows in Fig. 1 indicate the direction of increasing λ_0. In the following subsections, we discuss some interesting asymptotic limits of Eqs. (15).

A. Asymptotic Solutions In The Limit $|\lambda_0|\to\infty$

In Fig. 1, the point 0, from which both the T-branches emerge, corresponds to the limit $|\lambda_0|\to\infty$. The solid line designated by T, which extends from the origin to the point 0, is parametrized by $\lambda_0\varepsilon(0,+\infty)$. The dashed line, which starts from 0, extends upwards and is also designated by T, is parametrized by $\lambda_0\varepsilon(-\infty,0)$. In the limit $|\lambda_0|\to\infty$, if we define the parameter $\varepsilon \equiv 1/\lambda_0$, to leading order in ε, Eqs. (15) may be solved by a regular expansion in ε, i.e.,

$$\bar{B}_z = \sum_{n=0}^{\infty} \varepsilon^n \bar{B}_z^{(n)}, \tag{16}$$

etc. To 0(1), we then have

$$1 + 2(\bar{\Psi}(0) - \bar{\Phi}(0)) = 0, \tag{17}$$

which gives

$$q^{(0)} = d\Phi^{(0)}/d\Psi^{(0)} = q_s \ . \tag{18}$$

Thus, to leading order in ε, as we approach the point 0 in the T-branches, the q-profile tends to be constant everywhere in the plasma and precisely equal to the pitch of the dominant mode. Figs. (2e-h) show typical numerically determined profiles for $\bar{B}_z$, $\bar{B}_\theta$, $\bar{J}_z$ and q on the minimum-energy T-branch. All the solutions on this branch have q-profiles which are monotonically increasing and are hence tokamaklike. Furthermore, $q(r) > q_s$ (=1, for the m=1, n=1 mode), for all the solutions on this branch, which means that the singular surface for the dominant mode is removed from the final, relaxed state. This is consistent with experimental observations and theoretical models of m=1, n=1 sawtooth activity in tokamaks in which it is seen that when the value of q falls below one near the center of the plasma, a rapid internal disruption dominated by the m=1, n=1 mode ensues, flattening the current profile locally and raising the value of q at the center slightly above one.[12]

Using

$$\bar{\underline{J}} \times \bar{\underline{B}} = 0, \tag{19}$$

which is implied by Eqs. (15a) to (15c), and the boundary conditions (15f), we get

$$\bar{B}_z^{(0)}(r) = \frac{(q_s R)^2 \bar{B}_0}{(q_s R)^2 + r^2} , \tag{20a}$$

$$\bar{B}_\theta^{(0)}(r) = \frac{q_s R\, r \bar{B}_0}{(q_s R)^2 + r^2} , \tag{20b}$$

$$\bar{\Phi}^{(0)}(r) = \frac{(q_s R)^2 \bar{B}_0}{2} \ell n \frac{(q_s R)^2 + r^2}{(q_s R)^2} , \tag{20c}$$

$$\bar{\Psi}^{(0)}(r) = \frac{(q_s R)^2 \bar{B}_0}{2} \ell n \frac{(q_s R)^2 + r^2}{(q_s R)^2 + 1} , \tag{20d}$$

where

$$\bar{B}_0 \equiv \left[(q_s R)^2 \ell n \frac{(q_s R)^2 + 1}{(q_s R)^2} \right]^{-1} . \tag{20e}$$

It is readily seen that

$$V(\lambda_0) \equiv \frac{2W(\lambda_0)}{R(2\pi\Phi_p)^2} = 4 \int_0^1 dr\, r\, (\bar{B}_\theta^2 + \bar{B}_z^2) , \tag{21}$$

and

$$\frac{K_0(\lambda_0)}{R(2\pi\Phi_p)^2} = 2\int_0^1 drr\left(\frac{\overline{\Phi B}_\theta}{r} - \frac{\overline{\Psi B}_z}{R}\right). \tag{22}$$

For $|\lambda_0|\to\infty$ in particular, using solutions (20) we find the asymptotic vaules $V \to 2\bar{B}_0$, $R^{-1}K_0(2\pi\Phi_p)^{-2} \to (2q_sR)^{-1}$ for the point 0 in Fig. 1.

If we carry the regular expansion (16) to one further order in ε, we get

$$\bar{B}_z^{(1)}(r) = \frac{2q_sR}{\left[(qR)^2+r^2\right]^2} - \frac{3(q_sR)^3}{\left[(q_sR)^2+r^2\right]^3} + C_1 , \tag{23a}$$

$$\bar{B}_\theta^{(1)}(r) = -\frac{3(q_sR)^2 r}{\left[(q_sR)^2+r^2\right]^3} + \frac{C_1 r}{q_sR} , \tag{23b}$$

$$\bar{\Psi}^{(1)}(r) = 3/4\,\frac{(q_sR)^3}{\left[(q_sR)^2+r^2\right]^2} + \frac{C_1 r^2}{2} + C_2 , \tag{23c}$$

$$\bar{\Phi}^{(1)}(r) = 3/4\,\frac{(q_sR)^3}{\left[(q_sR)^2+r^2\right]^2} - \frac{q_sR}{(q_sR)^2+r^2} + \frac{C_1 r^2}{2} + C_2\ , \qquad (23d)$$

where C_1 and C_2 are arbitrary constants of integration, to be determined by the boundary conditions

$$\bar{B}_\theta^{(1)}(0) = 0,\ \bar{\Psi}^{(1)}(1) = 0,\ \bar{\Phi}^{(1)}(0) = 0 \text{ and } \bar{\Phi}^{(1)}(1) = 0. \qquad (24)$$

Of these boundary conditions, $\bar{B}_\theta^{(1)}(0) = 0$ is satisfied trivially, but the three remaining conditions give rise to an overdetermined set of algebraic equations. It is, therefore, impossible to satisfy the boundary conditions to $O(\varepsilon)$ by a simple regular expansion of the form given by Eq. (16). This suggests the existence of a boundary-layer(s) at an endpoint(s) of the interval $[0,1]$. For the boundary-layer analysis, it is convenient to omit Eq. (15c) in favor of Eq. (19); thus, the set of equations we attempt to solve comprise (15b,d-f) and (19) [which imply Eq. (15c)]. Explicitly,

$$\varepsilon\,\frac{d\bar{B}_z}{dr} = -\,\bar{B}_\theta\left[1+2(\bar{\Psi}-\bar{\Phi})\right]\ , \qquad (25a)$$

$$\frac{1}{2}\,\frac{d}{dr}\,(\bar{B}_z^2+\bar{B}_\theta^2) + \frac{\bar{B}_\theta^2}{r} = 0\ , \qquad (25b)$$

$$\frac{d\bar{\Psi}}{dr} = q_sR\bar{B}_\theta\ , \qquad (25c)$$

$$\frac{d\bar{\Phi}}{dr} = r\bar{B}_z \ , \tag{25d}$$

subject to the boundary conditions (15f). Since the solutions of Eqs. (23) to 0(1) in ε satisfy the boundary conditions, we subtract them from the total solutions at the outset by defining the tilded quantities

$$\bar{B}_z \equiv \bar{B}_z^{(0)} + \tilde{B}_z, \ \bar{B}_\theta \equiv \bar{B}_\theta^{(0)} + \tilde{B}_\theta, \ \bar{\Psi} \equiv \bar{\Psi}^{(0)} + \tilde{\Psi}, \ \bar{\Phi} \equiv \bar{\Phi}^{(0)} + \tilde{\Phi} \ . \tag{26}$$

Substituting the definitions (26) in Eqs. (25) and subtracting the equations determining the zeroth order solutions, we get

$$\varepsilon \frac{d\tilde{B}_z}{dr} = -2(\tilde{B}_\theta + \bar{B}_\theta^{(0)})(\tilde{\Psi}-\tilde{\Phi}) - \varepsilon \frac{d\bar{B}_z^{(0)}}{dr} \ , \tag{26a}$$

$$\frac{d}{dr}\left(\tilde{B}_z\bar{B}_z^{(0)} + \tilde{B}_\theta\bar{B}_\theta^{(0)} + \frac{\tilde{B}_z^2+\tilde{B}_\theta^2}{2}\right) + \frac{\tilde{B}_\theta^2+2\bar{B}_\theta^{(0)}\tilde{B}_\theta}{r} = 0 \ , \tag{26b}$$

$$\frac{d\tilde{\Psi}}{dr} = q_s R \, \tilde{B}_\theta \ , \tag{26c}$$

$$\frac{d\tilde{\Phi}}{dr} = r \, \tilde{B}_z \ , \tag{26d}$$

The boundary conditions on the tilded quantities are

$$\tilde{B}_\theta(0) = 0,\ \tilde{\Psi}(1) = 0,\ \tilde{\Phi}(0) = 0,\ \tilde{\Phi}(1) = 0 \quad . \tag{27}$$

We first explore the possibility of having only one boundary layer at r=1. (It will turn out to be the case which agrees with the numerical solutions). Equations (23a) to (23d) are the solutions for the outer region. Then, the boundary condition $\bar{\Phi}^{(1)}(0) = 0$ yields at once

$$C_2 = \frac{1}{4q_s R} \quad . \tag{28}$$

Since the boundary conditions on Ψ and Φ in the regular expansion (16) are violated ony at $O(\varepsilon)$, we have $\tilde{\Psi}$, $\tilde{\Phi} = O(\varepsilon)$. We define the strained variable y according to

$$r - 1 \equiv |\varepsilon|^\alpha y \ , \tag{29}$$

where α is an exponent to be determined, which implies

$$\frac{d}{dr} = |\varepsilon|^{-\alpha} \frac{d}{dy} \ . \tag{30}$$

Then, from Eqs. (25c) to (25d), we find that $\tilde{B}_\theta$, $\tilde{B}_z = O(|\varepsilon|^{1-\alpha})$. It is now easy to see from Eq. (25a) by a "dominant balance" argument that the only allowable value for the exponent α is 1/2. We define new variables Φ_1, Ψ_1 such that

$$\tilde{\Phi} \equiv \varepsilon\ \Phi_1 \ , \tag{31a}$$

and

$$\tilde{\Psi} \equiv \varepsilon \Psi_1 \ . \tag{31b}$$

In terms of these variables

$$\tilde{B}_\theta = \text{sgn } \varepsilon \frac{|\varepsilon|^{1/2}}{R} \frac{d\Psi_1}{dy} \tag{32a}$$

$$\tilde{B}_z = \text{sgn } \varepsilon \ |\varepsilon|^{1/2} \frac{d\Phi_1}{dy} \ . \tag{32b}$$

Substituting Eqs. (32) into Eqs. (25a)-(25b), and neglecting subdominant terms, we get, respectively,

$$\frac{d^2\Phi_1}{dy^2} + 2B_\theta^{(0)}(1) \ [\Psi_1 - \Phi_1] \simeq - \frac{dB_z^{(0)}(1)}{dr} \ , \tag{33a}$$

and

$$\frac{d^2\Phi_1}{dy^2} + \frac{1}{(q_s R)^2} \frac{d^2\Psi_1}{dy^2} \simeq 0 \ . \tag{33b}$$

For the homogenous part of the coupled Eqs. (33), we assume the solutions to be of the form $\exp(\mu y)$, which is substituted in these equations to obtain the linear algebraic system

$$\begin{bmatrix} \mu^2 - 2B_\theta^{(0)} & 2B_\theta^{(0)}(1) \\ \mu^2 & \dfrac{\mu^2}{(q_s R)^2} \end{bmatrix} \begin{bmatrix} \Phi_1 \\ \Psi_1 \end{bmatrix} = 0 , \qquad (34)$$

which has nontrivial solutions if and only if

$$\mu^2 \left[\mu^2 - 2B_\theta^{(0)} - 2B_\theta^{(0)}(1)(q_s R)^2 \right] = 0. \qquad (35)$$

Equation (35) may be trivially solved to give the four roots $\mu = 0, 0, \pm(2\bar{B}_0 q_s R)^{1/2}$. To complete the solution, we need the particular integrals for Eqs. (33); these are

$$\Psi_1 = 0, \qquad (36a)$$

$$\Phi_1 = \frac{1}{2\bar{B}_\theta(0)} \frac{d\bar{B}_z(0)}{dr}. \qquad (36b)$$

The double roots $\mu = 0$ and the particular integrals (36) all lead to solutions which are analytic in ε and are already included in the outer region solutions (23). The root $\mu = -(2\bar{B}_0 q_s R)^{1/2}$ is not permissible because $\exp(\mu y)$ diverges in the "distinguished limit" $\varepsilon \to 0$, $y \to -\infty$, which corresponds to the outer limit of the inner region. Thus, the solutions in the inner region are a linear combination of the outer region solutions which are analytic in ε and the solutions

$$\Psi_1 = C_3 \exp \left[(2\bar{B}_0 q_s R)^{1/2} y\right], \tag{37a}$$

$$\Phi_1 = -(q_s R)^2 \, C_3 \exp \left[(2\bar{B}_0 q_s R)^{1/2} y\right], \tag{37b}$$

which are non-analytic in ε, C_3 being an arbitrary constant. The two remaining constants C_1 and C_2 are determined from the two remaining boundary conditions, $\tilde{\Psi}(1) = 0$ and $\tilde{\Phi}(1) = 0$, which give

$$C_1 = -\frac{2(q_s R)^2 + 1}{2q_s R\left[(q_s R)^2+1\right]^2}, \tag{38a}$$

and

$$C_3 = \frac{q_s R}{\left[(q_s R)^2+1\right]^2}. \tag{38b}$$

We obtain, finally, in the limit $|\lambda_0| \to \infty$

$$\bar{\Psi}(r) \simeq \frac{(q_s R)^2 \bar{B}_0}{2} \ln \frac{(q_s R)^2 + r^2}{(q_s R)^2+1} + \frac{1}{\lambda_0} \left[\frac{C_1 r^2}{2} + \frac{1}{4q_s R} + \frac{3}{4}\frac{(q_s R)^3}{\left[(q_s R)^2+r^2\right]^2} - C_3 (q_s R)^2 \exp\left\{(2\bar{B}_0 q_s R|\lambda_0|)^{1/2}(r-1)\right\}\right] \tag{39}$$

and

$$\bar{\Phi}(r) \simeq \frac{(q_s R)^2 \bar{B}_0}{2} \ell n \frac{(q_s R)^2 + r^2}{(q_s R)^2} + \frac{1}{\lambda_0} \left[\frac{C_1 r^2}{2} + \frac{1}{4 q_s R} - \frac{q_s R}{(q_s R)^2 + r^2} \right.$$

$$\left. + \frac{3}{4} \frac{(q_s R)^3}{[(q_s R)^2 + r^2]^2} - C_3 (q_s R)^2 \exp \left\{ (2\bar{B}_0 q_s R |\lambda_0|)^{1/2} (r-1) \right\} \right] \quad , (40)$$

where C_1, C_2, C_3, and $\bar{B}_0$ are given, respectively, by Eqs. (38a), (28), (38b), and (20e). We may easily determine $\bar{B}_\theta(r)$ and $\bar{B}_z(r)$ by differentiating Eqs. (39) and (40) and using Eqs. (25c) and (25d). Indeed, these analytic solutions reproduce accurately numerically determined solutions on the T-branches in the vicinity of the point 0.

B. a/R - expansion

We now show that the solutions on the T-branch may be represented approximately by an expansion in a/R. We note at first that Eq. (12) may be written as the following system of two second-order equations:

$$\frac{d}{dx} \left(\frac{1}{x} \frac{d\Phi}{dx} \right) = -\varepsilon_0^2 \Lambda_0 \left[1 + \frac{q_s \Psi - \Phi}{\Phi_p} \right] \frac{d\Psi}{dx} \quad , \qquad (41a)$$

$$\frac{d}{dx} \left(x \frac{d\Psi}{dx} \right) = \Lambda_0 \left[1 + \frac{q_s \Psi - \Phi}{\Phi_p} \frac{d\Phi}{dx} \right] , \qquad (41b)$$

where $x \equiv r/a$, $\varepsilon_0 \equiv a/R$ and $\Lambda_0 = R\lambda_0$. The boundary conditions are

$$\Phi(0) = 0, \ \Phi(a) = \Phi_p \ , \qquad (42a)$$

$$\Psi(1) = 0, \quad \frac{d\Psi(0)}{dx} = 0 \ . \tag{42b}$$

We expand Φ and Ψ in the perturbation series

$$\Phi = \sum_{n=0}^{\infty} \varepsilon_0^{2n} \Phi^{(2n)} \ , \tag{43a}$$

$$\Psi = \sum_{n=0}^{\infty} \varepsilon_0^{2n} \Psi^{(2n)} \ . \tag{43b}$$

To O(1), Eq. (41a) may be integrated trivially. The result, which obeys the boundary conditions (42a), is

$$\Phi^{(0)}(r) = \Phi_p \frac{r^2}{a^2} \ , \tag{44}$$

which may be substituted in Eq. (41b) to give

$$\frac{d}{dx}\left[x \frac{d}{dx} \left\{\frac{\Psi^{(0)}}{\Phi_p}\right\}\right] - 2\Lambda_0 q_s x \left(\frac{\Psi^{(0)}}{\Phi_p}\right) = 2\Lambda_0 x(1-x^2). \tag{45}$$

Equation (45) may be solved by expanding in a complete set of eigenfunctions for the homogenous equation. This expansion is precisely

$$\Psi^{(0)}(x) = \Phi_p \sum_{n=1}^{\infty} a_n J_0 (k_n x), \tag{46}$$

where the sequence k_n satisfies

$$J_0(k_n) = 0. \tag{47}$$

Equations (46) and (47) insure that the boundary conditions (42b) are satisfied. The coefficients a_n may be determined by substituting the expansion (46) into Eq. (45); we get

$$a_n = - \frac{16\Lambda_0}{k_n^3 (k_n^2+2\Lambda_0 q_s)} \frac{1}{J_1(k_n)} \tag{48}$$

Therefore,

$$\Psi(0) = - 16R\lambda_0\Phi_p \sum_{n=1}^{\infty} \frac{1}{k_n^3(k_n^2+2R\lambda_0 q_s)} \frac{J_0(k_n r/a)}{J_1(k_n)} \tag{49}$$

From Eqs. (44) and (49), we get for a=1

$$\overline{B}_z(r) \simeq 1 \tag{50}$$

$$\overline{B}_\theta(r) \simeq \sum_{n=1}^{\infty} \frac{8\lambda_0}{k_n^2(k_n^2+2\lambda_0 q_s R)} \frac{J_1(k_n r)}{J_1(k_n)} . \tag{51}$$

It may be shown that the infinite series in (51) converges absolutely and uniformly[13]. Furthermore, since k_n determines zeros of J_0 and the denominator in the infinite series carries the term k_n^4, the series converges rapidly. In Figs. 3 and 4, we compare numerical solutions of $\overline{B}_\theta$ on the T-branches with the analytical approximation derived by retaining the first two terms of the series. Even for $\varepsilon_0 = 1$, the agreement is good, as is seen in Fig. 4.

We have so far discussed in detail those solutions of Eqs. (15) which are on the T-branches. As shown in Fig. 1, there are two P-branches, both of which are designated by P. The solid line is parametrized by $-2.5 < \lambda_0 < 0$ and the dashed line by $0 < \lambda_0 < 6.5$. In Paper I, we had made the claim that both the T- and the P-branches emerge from the point 0 on the presumption that 0 corresponds to the limit $|\lambda_0| \to \infty$ on all four branches. However, a more careful numerical search on the P-brances has not led to any solutions in the ranges $\lambda_0 < -2.5$, $\lambda_0 > 6.5$. We have not found by analysis of Eqs. (15) an obvious reason for this perplexing detail, but since it does not change the overall physical picture, we shall not dwell on it further. Figures (2a)-(2d) show $\bar{B}_z$, $\bar{B}_\theta$, $\bar{J}_z$ and q profiles for a typical equilibrium in the pinchlike window on the minimum energy P-branch. The q-profiles in this window are monotonically decreasing and reverse sign near the edge of the plasma.

The solutions on the T- and P-branches may be distinguished by their asymptotic behaviour for small λ_0. In the next subsection, we consider this asymptotic limit.

C. Asymptotic Solutions in the Limit $|\lambda_0| \to 0$

If $\lambda_0 = 0$, Eqs. (15) may be solved trivially to give

$$\bar{B}_z = 1, \ \bar{B}_\theta = 0, \ \bar{\Phi} = r^2/2, \text{ and } \bar{\Psi} = 0 \ , \tag{52}$$

for which $V(\lambda_0=0) = 2$ and $k_0(\lambda_0=0) = 0$. For $\lambda_0 \to 0$, the solutions on the T- and the P-branches have different asymptotic properties which may be understood by the following "dominant balance" argument. We assume that as $|\lambda_0| \to 0$, all solutions $\sim |\lambda_0|^\nu$. The term on the L.H.S. of Eq. (15b) or (15c) $\sim |\lambda_0|^\nu$, the first term on the R.H.S. $\sim |\lambda_0|^\nu$ and the second term $\sim |\lambda_0|^{2\nu+1}$. The method of dominant balance gives us two possible values of ν; $\nu = 0$,

which corresponds to balancing the L.H.S. against the first term on the R.H.S. and $\nu = -1$, which corresponds to balancing the L.H.S. against the second term on the R.H.S.

Here $\nu = 0$ describes the asymptotic behaviour of the T-branches for $|\lambda_0| \to 0$. The valid expansion for the solutions in this case is given by

$$\overline{B}_z = \sum_{n=0}^{\infty} \lambda_0^n \overline{B}_z^{(n)} ,$$

etc. The solutions, correct to $0(\lambda_0)$, are

$$\overline{B}_z(r) \simeq 1, \ \overline{B}_\theta(r) \simeq \frac{\lambda_0 r}{2}\left(1 - \frac{r^2}{2}\right), \ \overline{\Psi}(r) \simeq \frac{\lambda_0}{4}\left(r^2 - \frac{r^4}{4} - \frac{3}{4}\right)$$

and

$$\overline{\Phi}(r) \simeq r^2/2 , \tag{53}$$

and show good agreement with numerical solutions on the T-branches for small λ_0.

Here $\nu = -1$ describes the asymptotic behaviour of the P-branches for $|\lambda_0| \to 0$. The expansion in powers of λ_0 in this case is nonuniform and given by the series

$$\overline{B}_z = \sum_{n=-1}^{\infty} \lambda_0^n \overline{B}_z^{(n)} , \tag{54}$$

etc. To $0(\lambda_0^{-1})$, we have from the system of Eqs. (15)

$$\overline{B}_z^{(-1)\prime} = -2\overline{B}_\theta^{(-1)}\left[\overline{\Psi}^{(-1)} - \overline{\Phi}^{(-1)}\right], \tag{55a}$$

$$\frac{1}{r}\left[r\, \overline{B}_\theta^{(-1)} \right]' = 2\overline{B}_z^{(-1)}\left[\overline{\Psi}^{(-1)} - \overline{\Phi}^{(-1)} \right], \tag{55b}$$

$$\left[\overline{\Psi}^{(-1)}\right]' = q_s R \overline{B}_\theta^{(-1)} , \tag{55c}$$

$$\overline{\Phi}^{(-1)\prime} = r\overline{B}_z^{(-1)} , \tag{55d}$$

$$\overline{B}_\theta^{(-1)}(0) = 0,\ \overline{\Psi}^{(-1)}(1) = 0,\ \overline{\Phi}^{(-1)}(0) = 0,\ \overline{\Phi}^{(-1)}(1) = 0, \tag{55e}$$

where primes indicate differentiation with respect to r. To $0(1)$, we have similarly

$$\overline{B}_z^{(0)\prime} = -\overline{B}_\theta^{(-1)}\left[1+2\left(\overline{\Psi}^{(0)} - \overline{\Phi}^{(0)}\right)\right] - 2\overline{B}_\theta^{(0)}\left[\overline{\Psi}^{(-1)} - \overline{\Phi}^{(-1)}\right] , \tag{56a}$$

$$\frac{1}{r}\left[r\overline{B}_\theta^{(0)}\right]' = \overline{B}_z^{(-)}\left[1+2\left(\overline{\Psi}^{(0)} - \overline{\Phi}^{(0)}\right)\right] + 2\overline{B}_z^{(0)}\left[\overline{\Psi}^{(-1)} - \overline{\Phi}^{(-1)}\right] , \tag{56b}$$

$$\overline{\Psi}^{(0)\prime} = q_s R \overline{B}_\theta^{(0)} , \tag{56c}$$

$$\overline{\Phi}^{(0)\prime} = r\overline{B}_z^{(0)} , \tag{56d}$$

$$\bar{B}_\theta^{(0)}(0) = 0,\ \bar{\Psi}^{(0)}(1) = 0,\ \bar{\Phi}^{(0)}(0) = 0,\ \bar{\Phi}^{(0)}(1) = 1/2\ . \qquad (56e)$$

Therefore, the solutions on the P-branch are given approximately by

$$\bar{B}_z(r) \simeq \frac{\bar{B}_z^{(-1)}}{\lambda_0} + \bar{B}_z^{(0)}, \qquad (57)$$

etc. Equations (55) and (56), not essentially much simpler than Eqs. (15) from which they were derived, have been solved numerically. The numerical results, summed according to (57), show good agreement with numerical solutions of the P-branches for small λ_0. In Table I, we verify the λ_0^{-1} scaling of the solutions for small λ_0 by demonstrating, for instance, that the quantities $\lambda_0\bar{B}_z(1)$ and $\lambda_0\bar{B}_\theta(1)$ are approximately constant.

III. Comparison With Experimental Data on Self-Reversal in Pinches

In Fig. 5, we compare the $F - \Theta$ $\left[F = \bar{B}_z^{(1)},\ \Theta = \bar{B}_\theta(1)\right]$ predictions from the present theory with experimental data from Eta-Beta II.[14] We indicate the theoretical curve assuming the dominant mode to be m=1, n=1, which is also the mode for the numerical results reported earlier. As discussed earlier, this choice is appropriate for tokamaks. But for pinches, it is likely that the m=1, n=1 mode dominates in the very early phase of the discharge and is succeeded by m=1 modes of higher n-number such that the singular surface [defined by $q(r) = q_s$] corresponding to the dominant mode falls within the plasma during relaxation. The dashed line in Fig. 6 is the prediction from the theory assuming the dominant mode to be m=1, n=5 ($q_s = 0.2$). We note that the results of the theory do not change markedly. We have repeated

the calculations for a few other low n-numbers ($n \lesssim 10$), and have noticed some but not drastic movement of the value of Θ for null toroidal field. In Fig. 6, we show the graph of V vs. $R^{-1}K_0(2\pi\Phi_p)^{-2}$ for the m=1, n=5 mode. We note that the graph is very similar in structure to the one in Fig. 1 for the m=1, n=1 mode. The qualitative features of the tokamak-like and pinchlike profiles are also similar. Typically, since most toroidal devices in practice have aspect ratios from 3 to 10, and there are usually a few modes that are dominantly excited, we may conclude safely that the value of Θ at which the toroidal field reverses may vary to some extent from one experiment to the other depending on the aspect ratio of the device and the dominant resistive modes, but will, nevertheless, lie in a reasonably narrow window. Perhaps it should be emphasized here that agreement with F - Θ predictions from experiments is not a definitive test for the correctness of relaxation theories such as the present work or for that matter, Taylor's theory, the progenitor of much activity in this area. A more crucial test is the outcome of the computation, perhaps numerical, of the rate of decay of magnetic energy and the global invariants from the three-dimensional resistive magnetohydrodynamic equations.

IV. Stability of Minimum Energy Equilibria

The stability analysis is performed by means of a computer code which integrates Newcomb's Eq.[15] from the origin to the singular point where m=nq(r), and from the wall to the singular point, using an adaptive numerical integrator. (This is different from conventional reversed-field pinch terminology,[9] in which rational surfaces are defined by the relation m + nq(r) = 0. For both cases, $m \geq 0$ but the sign of n is opposite for the same value of q). The equilibrium magnetic fields $B_\theta(r)$ and $B_z(r)$ are fitted to cubic spline functions and then used to evaluate the coefficients of the differential equations. Ideal M.H.D.

instability is indicated if Suydam's criterion is violated at the singular point, or if the solution to Newcomb's equation passes through zero before reaching the singular point. As the solution approaches the singular point, it is fitted to analytically computed power series solutions. The ratio of the coefficients of the two independent solutions is computed , and the integration proceeds until convergence is obtained. The ratio on the left and right of the singular point are then used to compute the quantity Δ' of tearing mode stability theory.[16,17] A more detailed description of the code is given elswhere.[18]

Using the code described above, we have investigated the stability of the minimum energy equilibria lying on the T- and the P-branches (i.e., those equilibria lying on the solid lines in Fig. 1) to fixed-boundary low m and n ideal and resistive modes with singular surfaces inside the plasma. The reason for confining our attention to low m and n modes is twofold. First, the Kadomtsev-Monticello model, which guides our choice of global invariants, is primarily valid for m=1, n=1 modes in tokamaks, and the process of minimizing energy subject to invariants approximately preserved in a discharge dominated by a tearing instability of low mode number may be realistically expected to lead to equilibria stable to low m and n perturbations. Second, it is well known that the instabilities most deleterious to confinement are those with low mode numbers, and it is therefore sensible to investigate at first stability of any set of equilibria with respect to these modes.

The tokamaklike minimum energy equilibria, indicated by the solid T-line in Fig. 1, is tested for stability against the m=1 n=1, m=2 n=1, m=3 n=2, m=4 n=3, m=5 n=3, and m=7 n=4 modes. In Sec. I, we have shown by asymptotic analysis that for a tokamak discharge dominated by the m=1, n=1 mode, there is no singular surface with q=1 inside the plasma for solutions on the minimum energy T-branch. The stability of these equilibria to the other modes listed above may be summarized as follows. The

equilibria are all ideally stable to these modes. There is a window at $\Theta \sim a/R$, in which the equilibria are resistively stable to all but the m=3, n=2 mode. In Table II, we list the numerical results for a typical equilibrium (λ_0=1) from this window of stability.

From the work of Waddell, Carreras, Hicks and Holmes[7], we know that the most dangerous instability for a tokamak discharge is the m=2, n=1 mode which destabilized nonlinearly the m=3, n=2 mode and other higher harmonics, finally resulting in major disruptions. It has been emphasized[7] that the m=3, n=2 resistive mode, if present, may be innocuous by itself because it saturates at a low amplitude. These equilibria may thus be classified as non-disruptive, and perhaps describe relaxed states in a well-confined tokamak discharge.

This pinchlike equilibria, which lie on the solid line labelled by P and contain solutions with $q < 1$, monotonically decreasing and reversed on the outside are trivially stabilized with respect to the localized low m and n modes mentioned in the previous paragraph because there are no rational surfaces inside the plasma for those modes. However, rational surfaces are dense in such equilibria for m=1 modes of large n-number, and we have found our equilibria to be ideally unstable to such modes. The existence of these residual instabilities in a model of relaxation dominated by a tearing mode of single helicity is not surprising, and points towards the need for a global constraint better preserved than K_1 in strongly turbulent discharges such as those seen in reversed field pinches with slow current-rise.

Conclusion

In this paper, we have solved, numerically and analytically, for minimum-energy equilibrium states of a cylindrical plasma with no pressure. These equilibria have been constructed by minimizing

the total magnetic energy subject to a set of global constraints, which were recently proposed on the basis of a model of turbulent relaxation dominated by a tearing mode of single helicity. We have found both tokamaklike and pinchlike equilibria of minimum energy. We have examined these equilibria for ideal and resistive stability. It is found that the relaxed equilibria are always trivially stable to the assumed dominant mode. Furthermore, there is a narrow window of tokamaklike equilibria which are ideally stable to the important low m and n modes, but resistively unstable to the m=3, n=2 mode. For pinchlike equilibria, we have found residual high-n instabilities. In future work, we hope to remove the restriction of a dominant tearing mode of single helicity, and construct equilibria which are stable to a wider band of instabilities.

Acknowledgments

The first author (A.B.) would like to express his appreciation to Dr. D.A. Monticello and Dr. R.C. Grimm for stimulating discussions and criticism. He is grateful to M.J. Jirik for taking great pains over this manuscript.

This work was primarily supported by the United State Department Energy under Contract No. DE-FG05-80ET-53088 at the Institute for Fusion Studies, University of Texas at Austin, and Contract No. DE-AC02-76-CHO-3703 at the Plasma Physics Laboratory, Princeton University.

References

1. A. Bhattacharjee, R.L. Dewar, and D. A. Monticello, Phys. Rev. Lett. 45, 347(1980); Phys. Rev. Lett. 45, 1217(E)(1980).

2. A. Bhattacharjee and R.L. Dewar, Phys. Fluids 25, 887 (1982).

3. B. Kadomstev, Fiz. Flasmy 1, 710 (1975) [Sov. J. Plasma Phys. 1, 389 (1975)].

4. M. D. Kruskal and R. M. Kulsrud, Phys. Fluids, 1, 265 (1958).

5. J. B. Taylor, Phys. Rev. Lett. 35, 1139 (1974).

6. E. P. Butt, A. A. Newton, and A. J. L. Verhage, in Proceedings of the Third Topical Conference on Pulsed High Beta Plasmas, Culham Laboratory, United Kingdom, 1975, edited by D. E. Evans (Pergamon Press, 1976), p. 419.

7. B. V. Waddell, B. Carreras, H. R. Hicks, and J. A. Holmes, Phys. Fluids 22, 896 (1979).

8. H. P. Furth, P. H. Rutherford, and H. Selberg, Phys. Fluids 16, 1054 (1973).

9. D. C. Robinson, Nucl. Fusion 18, 939 (1978).

10. B. V. Waddell, M. N. Rosenbluth, D. A. Monticello, and R. B. White, Nucl. Fusion 16, 5 (1976).

11. J. C. Hosea, in Proceedings of the Workshop on Physics of Plasmas Close to Thermonuclear Conditions, Varenna, Italy, August 1979 (unpublished).

12. S. Von Goeler, W. Stodiek and N. Sauthoff, Phys. Rev. Lett. 33, 1201 (1974).

13. E. L. Ince, Ordinary Differential Equations (Dover Publications, First American Edition, 1927), pp. 254-278.

14. A. Buffa, S. Costa, R. De Angelio, L. Giudicotti, C. W. Gowors, G. F. Nalesso, S. Ortolani, M. Puiathi, P. Scarin, M.R.C. Watts, in Proceedings of the Reversed Field Pinch Theory Workshop (April 28, 1980), Los Alamos National Laboratory, Los Alamos, New Mexico.

15. W. A. Newcomb, Ann. Phys. 10, 232 (1980).

16. H. P. Furth, J. Killeen, and M. N. Rosenbluth, Phys. Fluids 6, 459 (1965).

17. A. H. Glasser, J. M. Greene, and J. L. Johnson, Phys. Fluids 18, 875 (1975).

18. M. S. Chance, H. P. Furth, A. H. Glasser, and H. Selberg, PPPL-1817, Plasma Physics Laboratory, Princeton University, Princeton, New Jersey 08544; submitted to Nucl. Fusion.

λ_0	$\lambda_0\bar{B}_z(1)$	$\lambda_0\bar{B}_\theta(1)$
0.1	0.41	-0.31
0.08	0.39	-0.31
0.06	0.37	-0.32
0.04	0.34	-0.33
0.02	0.32	-0.33
0.008	0.31	-0.34
0.005	0.30	-0.34
-0.06	0.22	-0.36
-0.04	0.25	-0.35
-0.02	0.27	-0.34
-0.008	0.28	-0.34
-0.006	0.29	-0.34
-0.004	0.29	-0.34
-0.002	0.29	-0.34

Table I Demonstration of the λ_0^{-1} scaling of the solutions on the P-branch for small λ_0.

Mode	Number	Position of singular surface	Ideal stability	Δ' Resistive stability
1	1	no singular surface	stable	stable
2	1	0.980	stable	-11.41, stable
3	2	0.741	stable	7.57, unstable
4	3	0.529	stable	-1.00, stable
5	3	0.854	stable	-4.60, stable
7	3	0.894	stable	-11.96, stable

Table II Ideal and resistive stability report for a typical solution (λ_0=1) in the minimum-energy windon on the T-branch.

Figure Captions

Fig. 1 Energy of equilibria in present theory compared with energy of axisymmetric equilibria in Taylor's theory (marked by Δ). Arrows indicate direction of increasing λ_0. Labels P and T distinguish pinchlike and tokamaklike equilibria. Dashed lines indicate equilibrium for which energy is stationary, but not minimum. The dominant mode is m=1, n=1.

Fig. 2 (a) $\overline{B}_z(r)$, (b) $\overline{B}_\theta(r)$, (c) $\overline{J}_z(r)$ and (d) q(r) for a solution on the minimum-energy P-branch. (e)$\overline{B}_z(r)$, (f) $\overline{B}_\theta(r)$, (g) $\overline{J}_z(r)$ and (h) q(r) for a solution on the minimum-energy T-branch. The dominant mode is m=1, n=1, and the aspect ratio is 5.

Fig. 3 Analytical approximation for $\overline{B}_\theta(r)$ compared with numerical result (q_s=1, λ_0=1, a/R=1/5) for typical tokamaklike equilibrium.

Fig. 4 Analytical approximation for $\overline{B}_\theta(r)$ compared with numerical result (q_s=1, λ_0=1, a/R=1) for typical tokamklike equilibrium.

Fig. 5 Comparison of theoretical predictions with F- Θ plot from ETA-BETA II.

Fig. 6 Energy of equilibria in present theory compared with energy of BFM (marked by Δ) assuming the dominant mode to be m=1, n=5. Dashed and solid lines have the same meaning here as in Fig. 1.

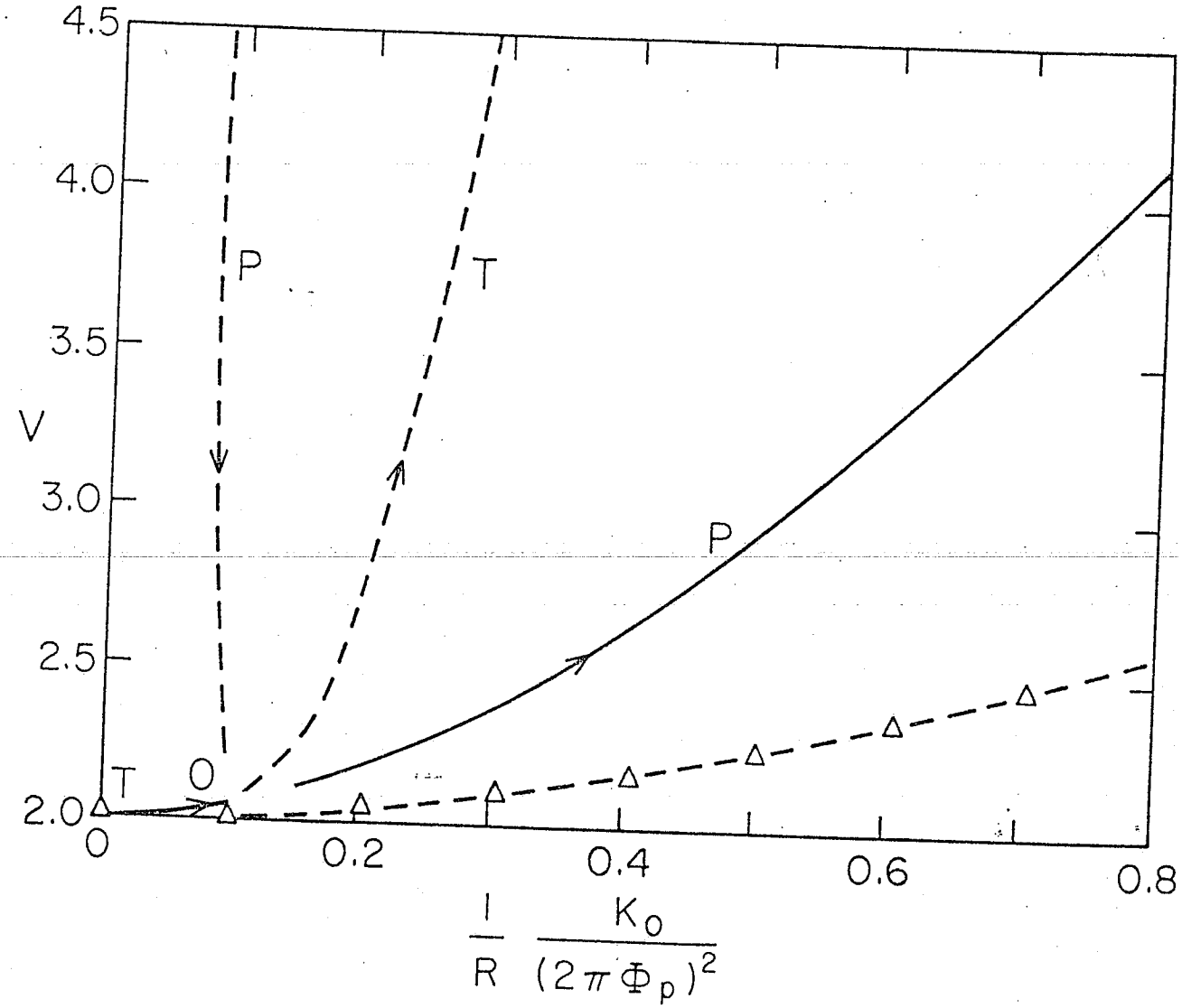

FIG. 1

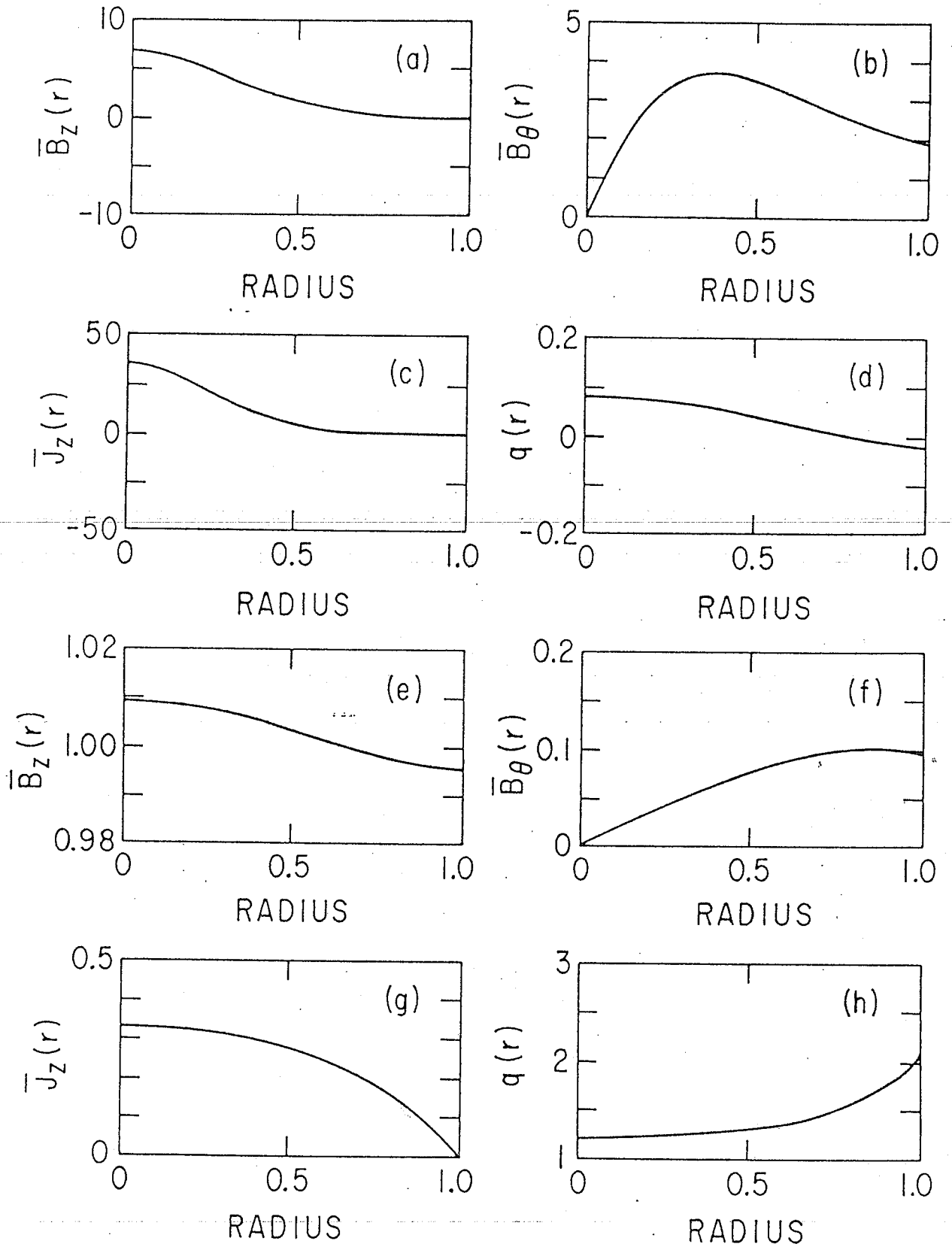
(a)
$\bar{B}_z(r)$
10
0
-10
0
0.5
1.0
RADIUS
(b)
$\bar{B}_\theta(r)$
5
0
0
0.5
1.0
RADIUS
(c)
$\bar{J}_z(r)$
50
0
-50
0
0.5
1.0
RADIUS
(d)
q(r)
0.2
0
-0.2
0
0.5
1.0
RADIUS
(e)
$\bar{B}_z(r)$
1.02
1.00
0.98
0
0.5
1.0
RADIUS
(f)
$\bar{B}_\theta(r)$
0.2
0.1
0
0
0.5
1.0
RADIUS
(g)
$\bar{J}_z(r)$
0.5
0
0
0.5
1.0
RADIUS
(h)
q(r)
3
2
1
0
0.5
1.0
RADIUS

FIG. 2

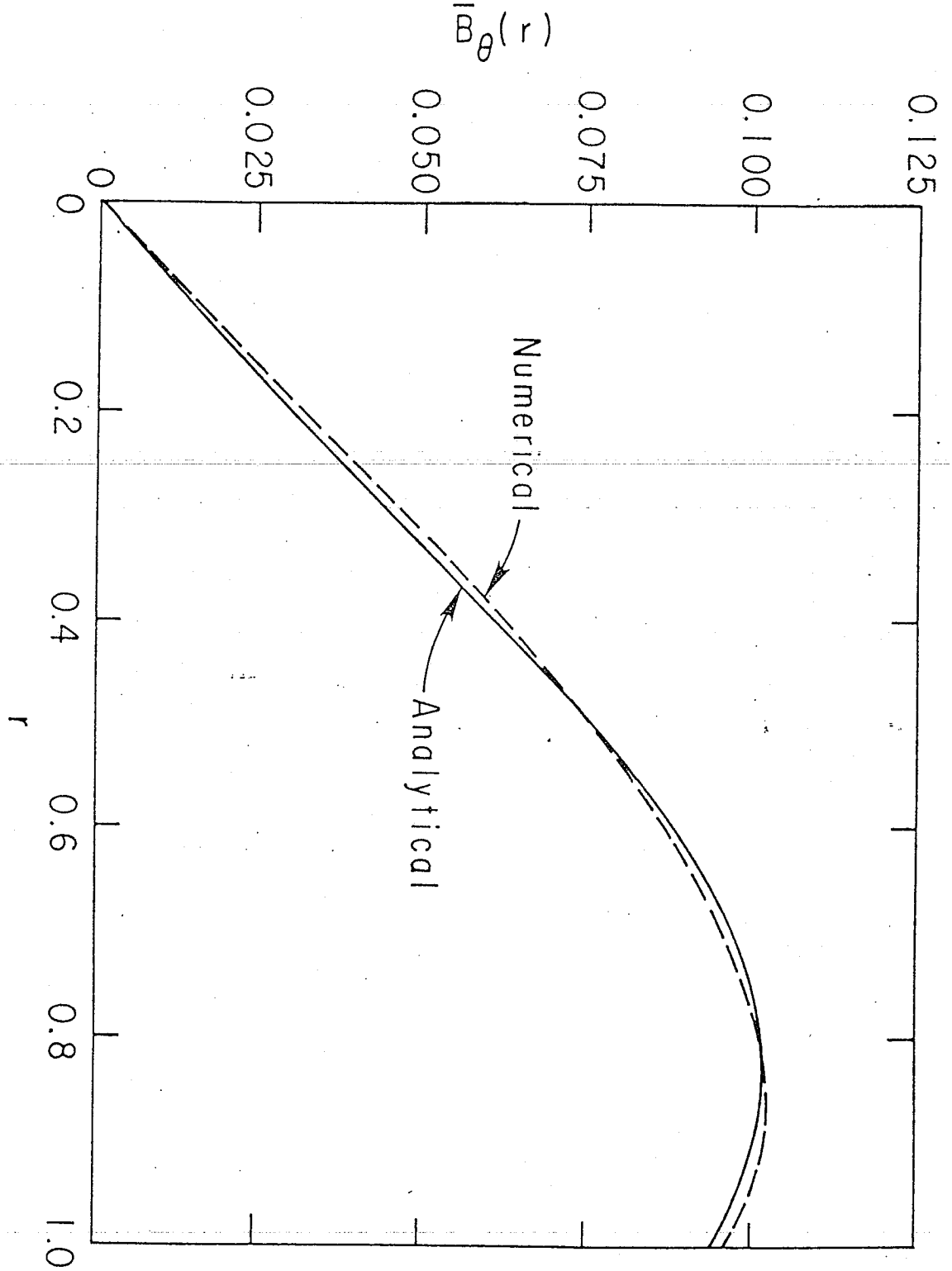
$\bar{B}_\theta(r)$
0.025
0.050
0.075
0.100
0.125
0
0
0.2
0.4
0.6
0.8
1.0
r
Numerical
Analytical

FIG. 3

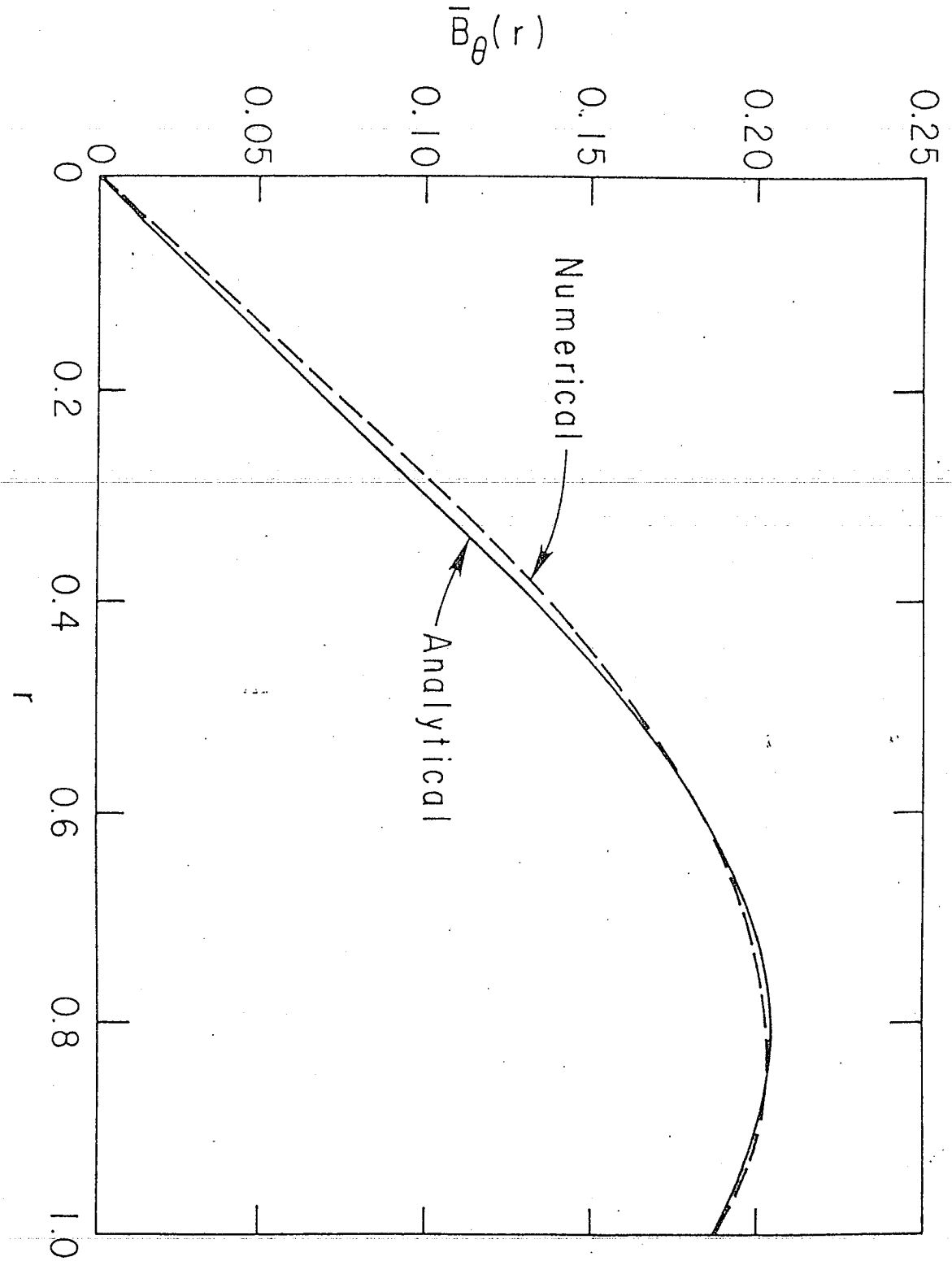
$\bar{B}_\theta(r)$
0
0.05
0.10
0.15
0.20
0.25
0
0.2
0.4
0.6
0.8
1.0
r
Numerical
Analytical

FIG. 4

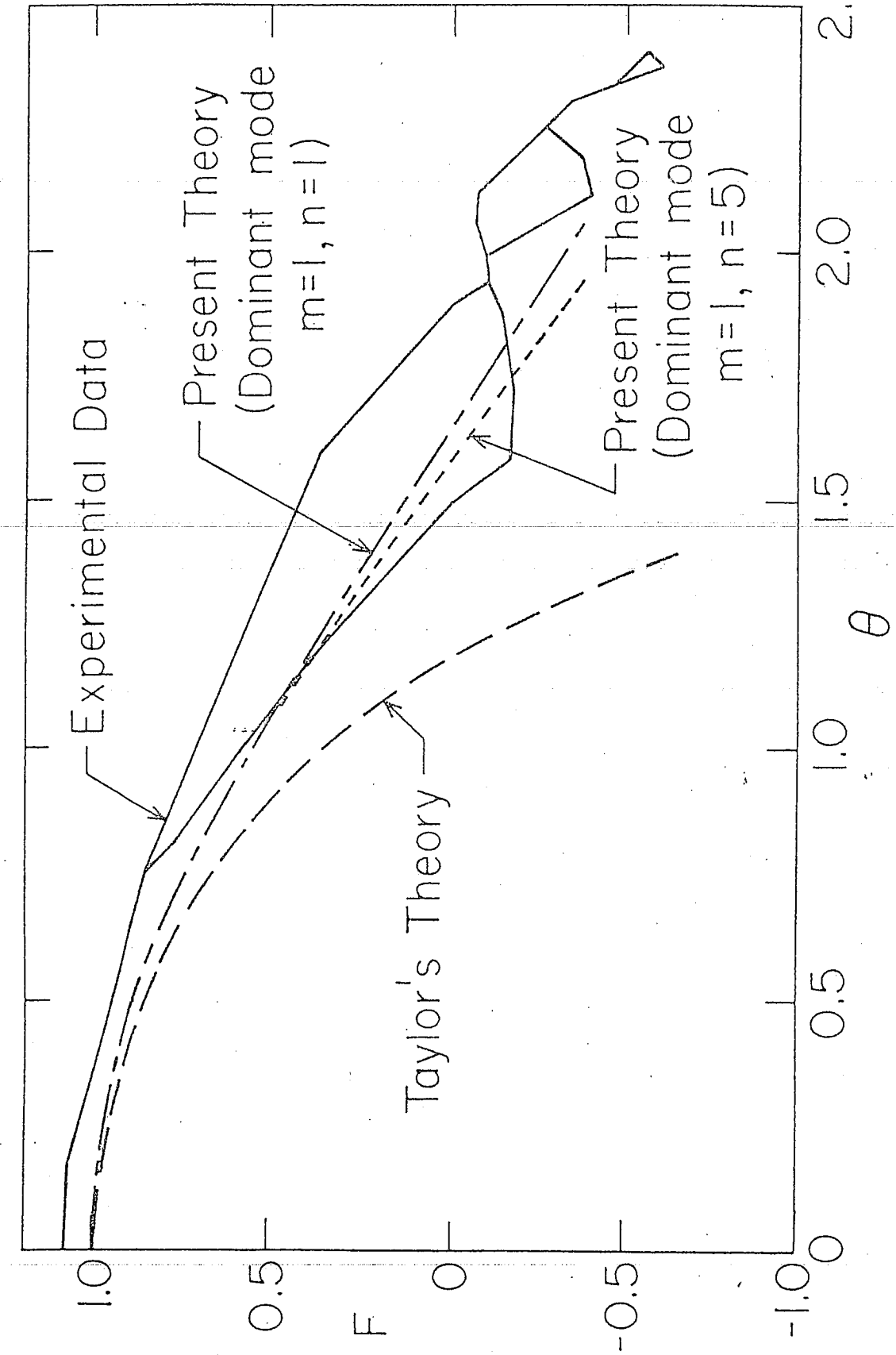
Experimental Data
Present Theory
(Dominant mode
m=1, n=1)
Present Theory
(Dominant mode
m=1, n=5)
Taylor's Theory
1.0
0.5
0
-0.5
-1.0
F
0
0.5
1.0
1.5
2.0
2.5
θ

FIG. 5

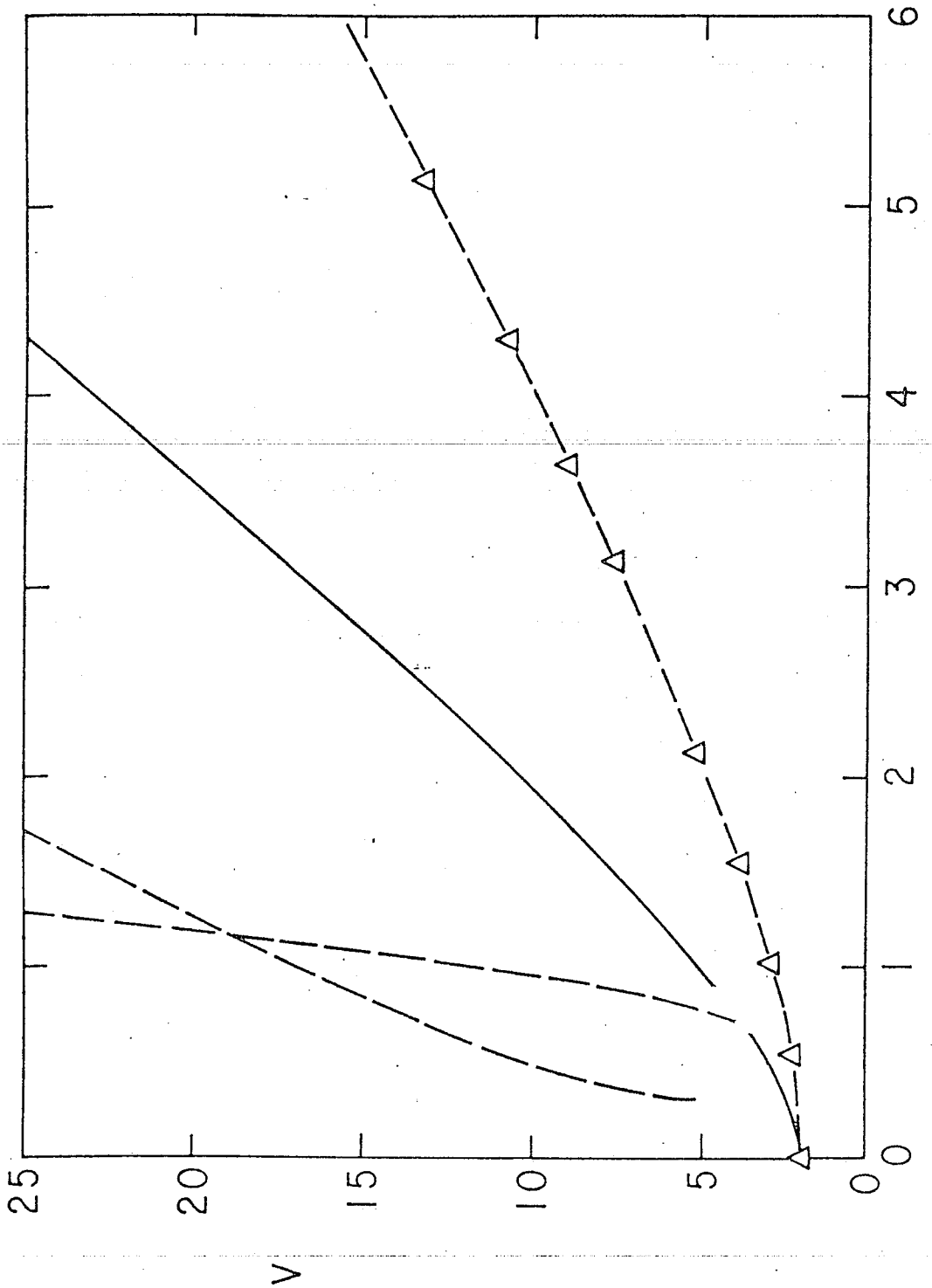

FIG. 6